Behavior and design of stainless steel tubular member welded end connections

Guven Kiymaz [*1] and Edip Seckin [2]

[1] *Department of Civil Engineering, Faculty of Engineering, Fatih University,*
Buyukcekmece Campus, Istanbul, Turkey
[2] *Department of Civil Engineering, Faculty of Engineering, Istanbul Kultur University,*
Atakoy Campus, İstanbul, Turkey

Abstract.   Among the various alternatives to make a steel tubular member connection, making a slotted and gusset plate welded connection is one of the most frequently preferred alternatives. This type of connection is essentially an end connection that is made by slotting the tube longitudinally, inserting the gusset plate and then placing longitudinal fillet welds at the tube-to-plate interface. In this paper an experimental study on the behaviour of such connections in stainless steel is presented. 24 specimens were tested under concentrically applied axial tensile forces for varying tube-to-gusset plate weld lengths. Both circular and box section members were considered in the test program. Load-deformation curves were obtained and comparisons were made in terms of strength and ductility. The results obtained from the study were then critically examined and compared with currently available design guidance for slotted gusset plate welded tubular end connections. It is noted that no specific rules exist in international specifications on structural stainless steel which cover the design of such connections. Therefore, the results of this study are compared with the existing design rules for carbon steel.

Keywords: stainless steel; tubular members; slotted and gusset plate welded connection; shear lag; tensile fracture

1. Introduction

The use of stainless steel in structural members of load-bearing systems has mostly been limited mainly due to cost considerations. These members have generally been preferred and used as secondary members in building structures with generally low structural capacity demand. Architectural concerns played an influential role in their preference and hence in real-life examples we have seen stainless steel members e.g., as load-carrying members of a building facade i.e., as exposed steel. On the other hand, the use of stainless steel in the main load-bearing elements of structural systems, e.g., building frames, may bring advantages in terms of issue regarding sustainability. Stainless steel with its favorable properties such as improved corrosion and fire resistance may provide possibilities for a more efficient balance between whole-life costs and in

---

∗Corresponding author, Associate Professor, E-mail: gkiymaz@fatih.edu.tr

service performance (Di Sarno *et al*. 2006). Combined with these advantages, its favorable strength and ductility properties would make stainless steel a material of choice in structural applications.

Relatively high initial cost of stainless steel is one burden for its structural use. To achieve a safe and economic design it is necessary to investigate the mechanical response of structural components, connections and the overall system, thus leading to efficient design (Di Sarno *et al*. 2006). With this respect, research studies on structural stainless steel (Afshan and Gardner 2013, Salih *et al*. 2013, Huang and Young 2013, Rossi and Rasmussen (2013), Theofanous and Gardner 2012, Feng and Young 2011, Nethercot *et al*. 2009, Baddoo 2008, Becque *et al*. 2008, Young 2008, Rasmussen *et al*. 2004, Aoki 2000, Burgan *et al*. 2000, Johansson and Olsson 2000, Khohi *et al*. 2000) has mostly covered issues that focus on more suitable design of structural stainless steel members and their connections.

The present paper aims to contribute to the above need for structural research for stainless steel and focuses on the specific subject of the behavior of slotted and gusset plate welded connections in stainless steel tubular members. Tubular members are among the most preferred member types used in structural stainless steel applications due to both their structural efficiency and attractive appearance. Hence using tubular members in stainless steel has been an architectural preference in many practical applications. Among the various alternatives of making a steel tubular connection, slotted and gusset plate welded connections is one way. As shown in Fig. 1 the end connection is made by slotting the tube longitudinally, inserting the gusset plate and then placing longitudinal fillet welds at the tube-to-plate interface.
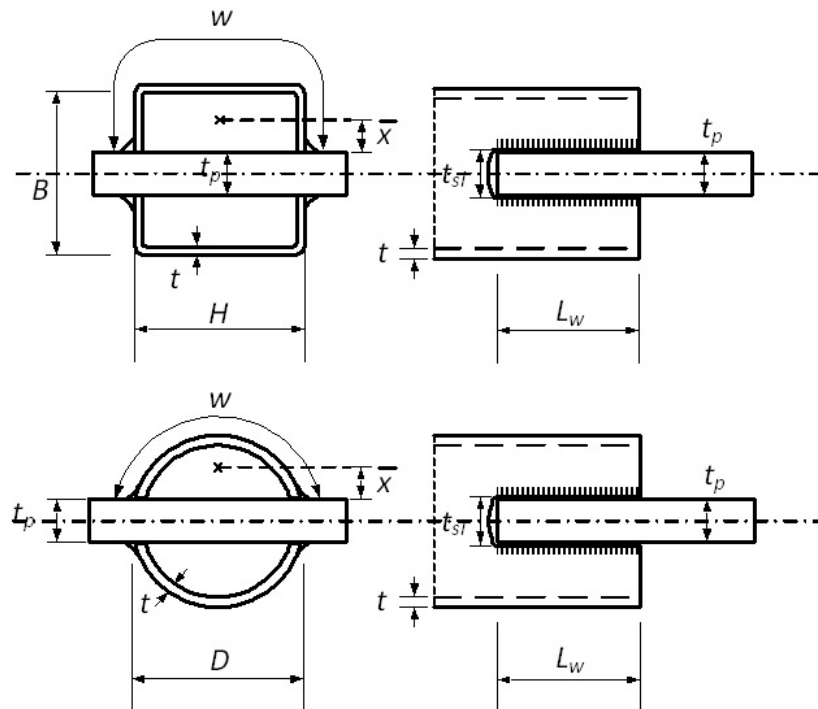

Fig. 1 Schematic view for the gusset plate welded slotted end connections for box and circular section members
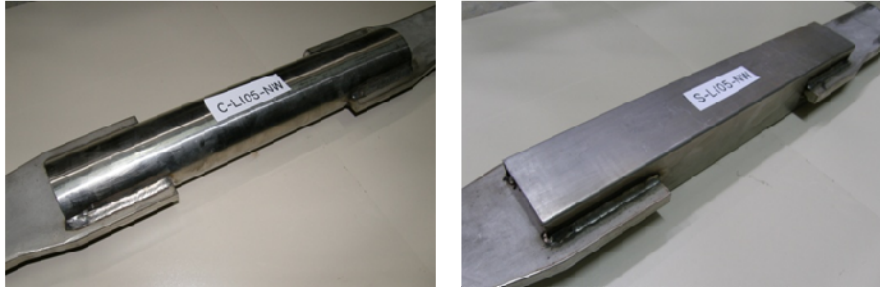
Fig. 2 View of the tested specimens in CHS and SHS

Fig. 3 View of the slot end conditions with / without a return weld

The research presented in this paper has studied the behaviour and design of such connections of stainless steel circular and square hollow section (CHS/SHS) members under static axial tensile loading. Experiments were conducted on slotted and gusset plate welded tubular member connections in stainless steel. Both circular and box section members were considered in the test program. 24 specimens were tested under concentrically applied axial tensile forces for varying tube-to-gusset plate weld lengths. Load-deformations curves were obtained and comparisons were made in terms of strength and ductility. The results obtained from the study were then critically examined and compared with currently available design guidance for slotted gusset plate welded tubular end connections. It is noted that no specific rules exist in international specifications on structural stainless steel which cover the design of such connections. Therefore, the results of this study are compared with the existing design rules for carbon steel.

2. Experimental study

2.1 Description of the tests and specimens

The study focuses on the behavior of slotted and gusset plate welded stainless steel tubular member connections subject to concentric axial loading. As stated earlier tests were carried out on 24 stainless steel CHS and SHS members with slotted gusset plate welded end connections. Fig. 2 shows photographs of two typical test specimens. Two parameters that were considered as

variables in the test program were the fillet weld length L_w and the end condition of the welded gusset plate inside the slot being welded or non-welded around the end face of the gusset plate. These end conditions are shown in Fig. 3. The welded end is denoted as RW (return weld) and the non-welded end is denoted as NW (no return weld).

As shown in the photographs given in Figs. 2 and 3 rigid gusset plates with 15 mm plate thickness were welded into the slots at both ends of the specimen. Tensile load was applied via these plates which were gripped inside the grip locations within the universal test machine with a total capacity of 50 tons. Loading was applied in the direction of the longitudinal axis of the member as concentric axial tensile load and specimen longitudinal elongation was monitored and recorded by using two displacement transducers attached to the sides of the specimen. Specimen dimensions are reported in Table 1. In the specimen reference, *C* stands for Circular and *L* defines

Table 1 Dimensional properties of the test specimens

Specimen	w (mm)	$\bar{x}$ (mm)	L_W (mm)	$\bar{x}/L_W$	L_W/w	L_W/D or L_W/H
C-L30-RW	104.54	24.22	30	0.81	0.29	0.39
C-L45-RW	104.54	24.22	45	0.54	0.43	0.59
C-L60-RW	104.54	24.22	60	0.40	0.57	0.79
C-L76-RW	104.54	24.22	76	0.32	0.73	1.00
C-L90-RW	104.54	24.22	90	0.27	0.86	1.18
C-L105-RW	104.54	24.22	105	0.23	1.00	1.38
C-L30-NW	104.54	24.22	30	0.81	0.29	0.39
C-L45-NW	104.54	24.22	45	0.54	0.43	0.59
C-L60-NW	104.54	24.22	60	0.40	0.57	0.79
C-L76-NW	104.54	24.22	76	0.32	0.73	1.00
C-L90-NW	104.54	24.22	90	0.27	0.86	1.18
C-L105-NW	104.54	24.22	105	0.23	1.00	1.38
S-L30-RW	122.42	26.25	30	0.88	0.25	0.43
S-L45-RW	122.42	26.25	45	0.58	0.37	0.64
S-L60-RW	122.42	26.25	60	0.44	0.49	0.86
S-L70-RW	122.42	26.25	70	0.38	0.57	1.00
S-L90-RW	122.42	26.25	90	0.29	0.74	1.29
S-L105-RW	122.42	26.25	105	0.25	0.86	1.50
S-L30-NW	122.42	26.25	30	0.88	0.25	0.43
S-L45-NW	122.42	26.25	45	0.58	0.37	0.64
S-L60-NW	122.42	26.25	60	0.44	0.49	0.86
S-L70-NW	122.42	26.25	70	0.38	0.57	1.00
S-L90-NW	122.42	26.25	90	0.29	0.74	1.29
S-L105-NW	122.42	26.25	105	0.25	0.86	1.50

CHS diameter, D = 76.1 mm, CHS thickness, t = 2.0 mm
SHS width, H = 70 mm, SHS thickness, t = 2.0 mm
Gusset plate thickness, t_p = 15 mm constant

the length of weld. $\bar{x}/L_w$, L_w/w and L_w/D ratios are all called weld length ratios used in the design calculations as described above. Five different weld lengths were considered starting from 30 mm up to 105 mm. For each cross-section type (CHS and SHS) 5 specimen were without a return weld (NW) and the other 5 with a return weld (RW) at the slotted end. For CHS sections a constant diameter of $D = 76.1$ mm and thickness of $t = 2.0$ mm was used for all the specimens tested whereas the SHS sections were all 70 mm × 70 mm square sections with wall plate thickness of $t = 2.0$ mm.

Table 1 presents the dimensional properties for the 24 specimens tested in the test program. Note that the notations are described in Fig. 1. Within the specimen designation the *C* stands for Circular and *S* for Square. The following, e.g., L60-RW corresponds to a longitudinal weld length of 60 mm with a Return Weld at the end. A constant weld thickness of 6 mm was considered in the production of the test specimen.

2.2 Material property tests

Tensile tests were carried out on tensile test coupons cut out from randomly selected tube members to determine the material property of the stainless steel used. The nonlinear behaviour of stainless steel material is generally described by the compound Ramberg-Osgood stress-strain expressions (Ramberg and Osgood 1943, Rasmussen 2003) as given below.

$$\varepsilon = \begin{cases} \dfrac{\sigma}{E} + 0.002\left(\dfrac{\sigma}{\sigma_{0.2}}\right)^n & \text{for } \sigma \ll \sigma_{0.2} \\[4mm] \dfrac{(\sigma - \sigma_{0.2})}{E_{0.2}} + \varepsilon_u\left(\dfrac{\sigma - \sigma_{0.2}}{\sigma_u - \sigma_{0.2}}\right)^m + \varepsilon_{0.2} & \text{for } \sigma_{0.2} < \sigma \ll \sigma_u \end{cases}$$

Properties determined from the recorded stress–strain relationship are E_0, $\sigma_{0.01}$, $\sigma_{0.2}$, σ_u, ε_u, n, m. where e is the nominal strain, σ is the corresponding nominal stress, $\sigma_{0.2}$ is the 0.2% proof stress, $\varepsilon_{0.2}$ is the total strain at the 0.2% proof stress, ε_u is the strain at the ultimate stress σ_u, E_0 is the initial Young's modulus, $E_{0.2}$ is the tangent stiffness at the 0.2 proof stress and n and m are the strain hardening exponents as given below.

$$n = \frac{\ln(20)}{\ln(\sigma_{0.2}/\sigma_{0.01})}$$

$$m = 1 + 3.5\frac{\sigma_{0.2}}{\sigma_u}$$

$$\frac{\sigma_{0.2}}{\sigma_u} = 0.2 + 185\frac{\sigma_{0.2}}{E_0}$$

$$E_{0.2} = \frac{E_0}{1 + 0.002n/e}$$

$$\varepsilon_{0.2} = \frac{\sigma_{0.2}}{E_0} + 0.002$$

Table 2 Measured material properties from tensile coupon tests

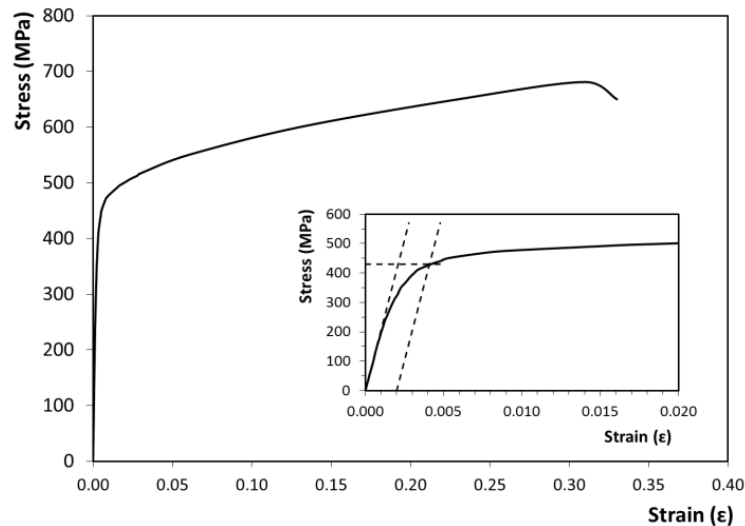| Specimen	E_0	$\sigma_{0.01}$	$\sigma_{0.2}$	σ_u	ε_u	n	m
TC01	205000	240	430	681	36,86	5,14	3,21
TC02	197000	300	425	657	35,31	8,6	3,26
TC03	200000	250	440	706	37,68	5,3	3,18
TC04	195000	150	315	670	52,99	4,04	2,65
TC05	190000	152	295	650	54,62	4,52	2,59
TC06	196000	140	275	630	56,35	4,44	2,53
TC07	203000	170	400	716	44,13	3,5	2,96
TC08	198000	140	410	714	42,58	2,79	3,01
TC09	197000	150	400	705	43,26	3,05	2,99

Fig. 4 Typical stress–strain curve from tensile coupon tests

$$\varepsilon_u = 1 - \frac{\sigma_{0.2}}{\sigma_u}$$

The material properties from the tensile tests are presented in Table 2. A typical stress–strain curve obtained from the tensile coupon tests is shown in Fig. 4. Note that a rounded material behavior is observed with no well-defined yield point. In calculating the design strength of the end connections of the specimens, the average values of 0.2% proof stresses ($\sigma_{0.2}$) and of the ultimate tensile stresses (σ_u) in Table 2 were used. These average values for $\sigma_{0.2}$ and σ_u are calculated as 380 MPa and 680 MPa, respectively.

3. Test results

3.1 General behavior under axial tensile loading

Experiments were carried out as described above for the 24 different specimens with varying connection configurations. The three possible failure modes that would be expected for the members with slotted end connections are yielding of the member gross cross-section (GY), block tear out of material close to the weld region (TO) and shear lag failure with fracture of the effective net cross section around the periphery of the member (PF). For the specimens in the test program no gross-section yielding was observed. On the other hand most of the specimens were observed to fail by peripheral fracture (PF) due to shear lag. Fig. 5 shows typical connection failures for a CHS and SHS section connection in a peripheral fracture mode. Specimens with longer weld lengths (particularly $L_w = 90$ mm and $L_w = 105$ mm) exhibited a nearly perfect peripheral fracture of the whole circular/square hollow cross section with crack propagating around the member periphery. For the specimens with shorter weld lengths (L_w between 30 mm and 70 mm) peripheral fracture which initiated at the slotted end and gusset plate juncture seemed later to interact with a tear out type of behavior. Compared with the long weld length specimens this behavior was accompanied with a relatively higher distortion of the end cross section and also at post peak loads longitudinal weld or tube material tearing (Fig. 6).

Fig. 7 shows close-up views of the failed specimens around the slotted end region both for "Return Weld (RW)" and "No Return Weld (NW)" cases. In both cases fracture initiated at the slotted end region due to high stress concentrations. For the NW cases, crack initiation was relatively easier in comparison to the RW (return weld) cases where the tensile load was at some point high enough to initiate a crack with the return weld material (photo on the left).

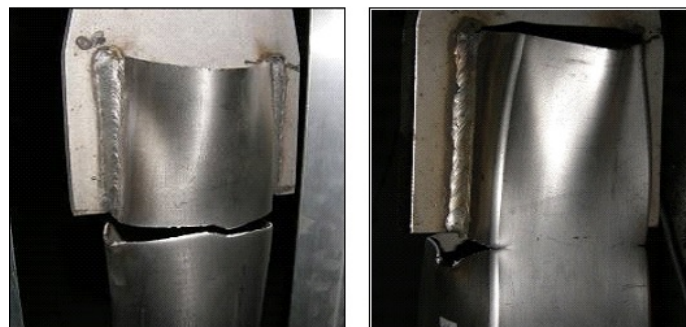Fig. 5 Typical deformed shapes observed for CHS and SHS members with long weld lengths

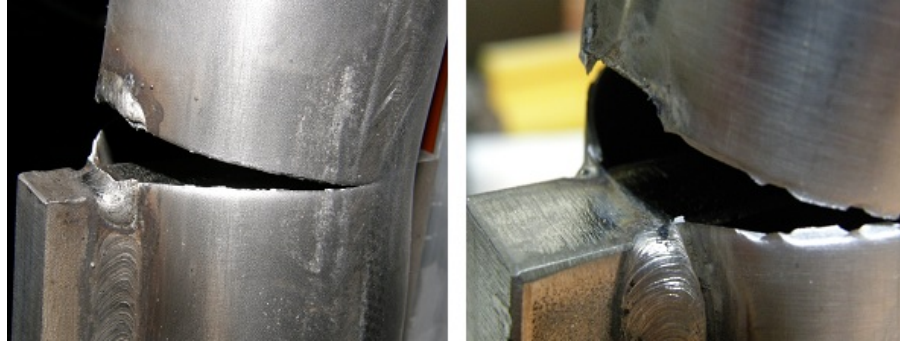Fig. 6 Typical deformed shape for short and medium weld length connections

Fig. 7 Failure types for return weld (RW) and no-return weld (NW) cases

3.2 Load-displacement response

Figs. 8 and 9 present the load displacement response curves for the NW and RW cases for both SHS and CHS sections, respectively. In general the behavior of the RW and the NW specimens are similar with close initial stiffness values and a rounded overall load-displacement response. However, for the RW cases for all the 6 specimens for both SHS and CHS members a sudden drop in strength is observed right after the maximum load is achieved whereas for the NW specimens a smooth transition is noted. For all the RW specimens the maximum load levels after which a sudden drop is observed correspond to load levels at which crack initiation was observed to occur during the tests within the return weld material. In other words, as soon as the return weld cracked a sudden drop in load occurred. On the other hand for the "No return weld" specimens, load was not as sensitive to the crack initiation which started directly on the CHS member material near the slotted end – gusset plate juncture where there is no return weld. With this respect, a more ductile behavior is observed for the specimens with their slotted ends un-welded to the gusset plate. In general the RW specimens reached higher ultimate loads than the NW specimens.
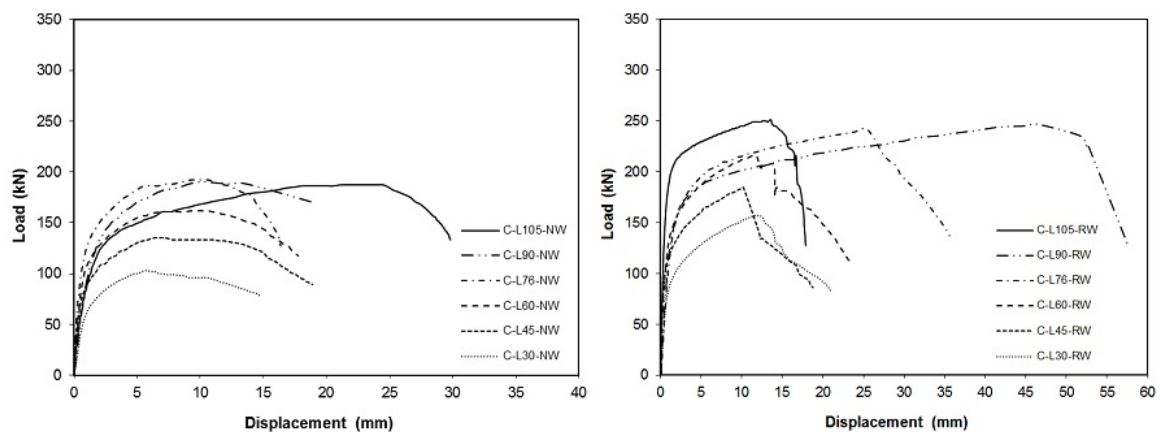

Fig. 8 Load-displacement curves for the 'No Return weld (NW) and with return weld (RW)'
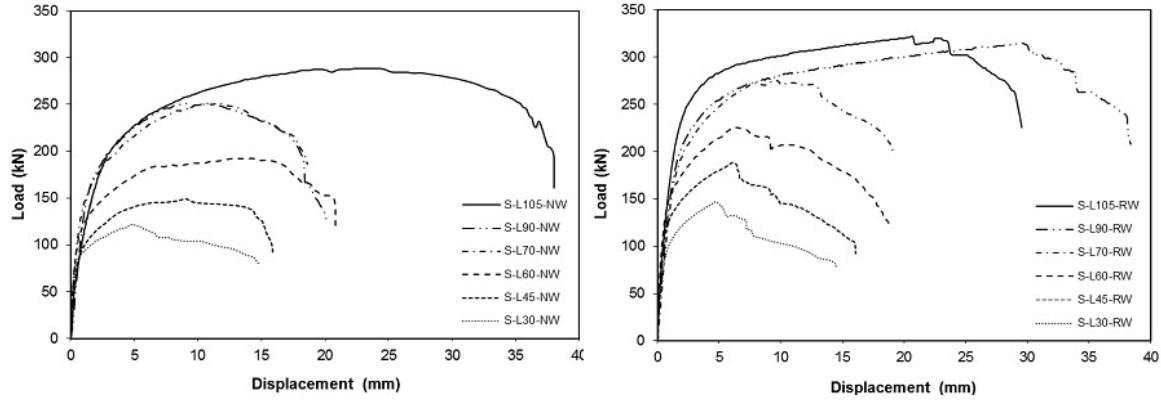specimens for Circular Hollow Sections

Fig. 9 Load-displacement curves for the 'No Return weld (NW) and with return weld (RW)' specimens for Square Hollow Sections

3.3 Strength of slotted end connections

3.3.1 Connection Yield Capacity Point (YCP)

As evidenced by the load-displacement response curves and visual observations made on the specimens, all the slotted gusset plate connections achieved their maximum strength after high deformations which create excessive distortions in the geometry of the connection. In order to prevent this impractical behaviour a serviceability limit should be applied in design. Therefore for design purposes which would also take into account of such serviceability limitations a lower test strength value than the peak test strength value is suggested to be applied. For this purpose a first yield approach is adopted to calculate the design strength levels. For all specimen tests a yield capacity point (YCP) is identified on the test load-displacement plots by using the equal area rule that is often used to estimate the yield point of a bilinear capacity curve that approximates a curvilinear one. As shown in Fig. 10 the connection yield capacity point calculated in this way is denoted by Q_y.
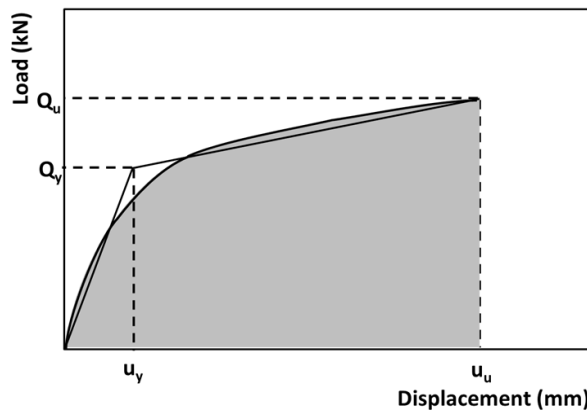

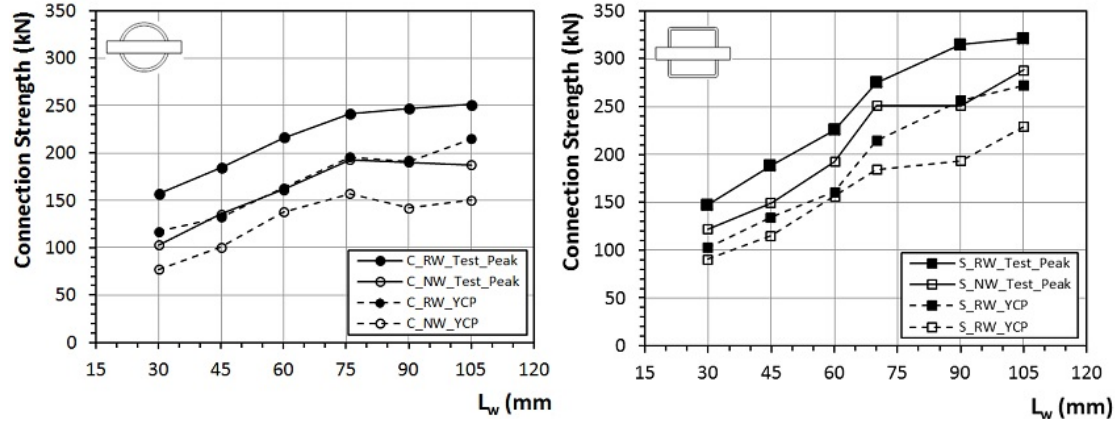Fig. 10 Determination of the connection yield capacity point, Q_y

Fig. 11 Variation of connection yield capacity point, Q_y and test peak strengths, N_{test} with weld length, L_w

Table 3 Peak and yield capacity strengths achieved for the CHS connections with corresponding elongations and failure modes

Specimen	N_{test} (kN)	δ_{test} (mm)	Q_y (mm)	δ_{Qy} (mm)	Test failure mode
C-L30-RW	157.0	12.2	117	1.17	TO
C-L45-RW	184.4	10.2	132	0.53	TO
C-L60-RW	215.8	11.8	163	0.75	TO
C-L76-RW	241.3	25.5	195	1.95	PF
C-L90-RW	247.2	46.3	191	1.43	PF
C-L105-RW	251.1	13.6	215	0.72	PF
C-L30-NW	103.0	5.7	77	1.15	TO
C-L45-NW	135.4	7.2	101	0.50	TO
C-L60-NW	161.9	10.6	138	0.92	TO
C-L76-NW	192.3	10.7	157	0.63	PF
C-L90-NW	190.3	10.3	142	1.42	PF
C-L105-NW	187.4	24.5	150	1.20	PF

3.3.2 Variation of strength with weld length

In Fig. 11 variation of the achieved test peak strength values (N_{test}) and the above explained yield capacity values (Q_y) is presented for the range of weld lengths studied both for circular and square hollow section specimens. In general for all the specimens connection strength increases with increasing weld length. The rate of increase in strength values with increasing weld lengths is greater for the SHS member connections. On the other hand for CHS connections, for weld lengths higher than $L_w = D = 76.1$ mm a nearly constant connection strength is achieved both for test peak and yield capacity levels.

Tables 3 and 4 present peak (N_{test}) and yield capacity strengths (Q_y) achieved for CHS and SHS connections with corresponding elongations (δ_{test} and δ_{Qy}) and failure modes. As explained earlier and shown in Figs. 5 and 6, test failure modes were either a PF (Peripheral Fracture) or a TO (Tear-out) mode where TO mode in fact corresponds to a combination of a PF mode and a tear-out

Table 4 Peak and yield capacity strengths achieved for the SHS connections with corresponding elongations and failure modes

Specimen	N_{test} (kN)	δ_{test} (mm)	Q_y (mm)	δ_{Qy} (mm)	Test failure mode
S-L30-RW	147.2	4.7	103	0.52	TO
S-L45-RW	188.4	6.1	135	0.54	TO
S-L60-RW	225.6	6.4	161	0.64	TO
S-L70-RW	274.7	9.8	214	1.46	PF
S-L90-RW	314.9	29.5	256	1.71	PF
S-L105-RW	321.8	20.7	272	1.60	PF
S-L30-NW	121.6	4.8	91	0.30	TO
S-L45-NW	149.1	9.1	115	0.58	TO
S-L60-NW	192.3	14.4	157	0.63	TO
S-L70-NW	251.1	11.7	184	0.74	PF
S-L90-NW	251.1	9.1	193	1.54	PF
S-L105-NW	288.4	24.3	229	1.53	PF

failure for short and medium weld length connections.

Considering all 24 specimens, the yield capacity strength levels (Q_y) correspond to around 75 percent of the test peak strengths (N_{test}). On the other hand, elongation levels corresponding to the yield capacity strength levels (δ_{Qy}) is in average 8 percent of the levels corresponding to the peak strength levels (δ_{test}). Among all the elongations achieved maximum value for δ_{Qy} is 1.95 mm whereas for δ_{test} a maximum elongation value of 46.3 mm is obtained. From the viewpoint of serviceability considerations discussed earlier the elongation levels corresponding to the yield capacity strength levels appear to be more reasonable values compared with those corresponding to the peak strength levels.

4. Design of slotted and gusset plate welded connections in stainless steel

The resistance of a steel tension member is given as the minimum of the resistance in yielding of the gross section area ($P_n = F_y.A_g$) and the resistance in fracture of an effective net section area (A_e) within the connection region ($P_n = F_u.A_e$). The effective area is used to determine the efficiency of the connection under the effects of shear lag and calculated by using a shear lag reduction coefficient, *U*. Design rules related to failure of slotted end tension connections with welded gusset plates can be found in three major international specifications on steel structures namely the American ANSI/AISC 360 (2010), the Canadian CAN/CSA-S16 (2009) and the European EN1993-1-8 (2005). Design methods adopted in these specifications are shown in Table 5 and Table 6 for shear lag and block shear tensile fracture (tear-out) failures respectively. Note that in EC3 Part 1.8 there are no design provisions for shear lag effect for such connections in hollow sections. In this design guide, rules for shear lag effect is given only for bolted connections for angles connected by one leg and other unsymmetrically connected tension members. Comparing the approaches adopted in these codes it is noted that for block shear failure the three codes present similar resistance equations. Nominal resistances predicted by these codes are equal

(a slightly different value predicted by EC3 in which shear yield coefficient is taken as the theoretical $1/\sqrt{3}$ value) but the design resistance values differ due to different resistance factors adopted in each code. However, it should be noted that in the block shear design equation of CAN/CSA-S16 (2009), the multiplication of two factors (0.85 and 0.90) equals 0.765 which is very close to the resistance factor used in the design equation of AISC (2010) which is 0.75. On the other hand, the resistance factor adopted in EN1993-1-8 (2005) is $1/\sqrt{1.25}$ which is again equal to a close value of 0.80. As for shear lag effect two general approaches are adopted. As presented in Table 5, shear lag coefficient, U, is calculated as a function of the ratio of the eccentricity of the connection ($\bar{x}$) to the weld length (L_w) in the American specification whereas in the Canadian specification U is a function of the ratio of the weld length (L_w) to peripheral distance between the welds (w). In both specifications the adverse effect of shear lag decreases as weld length L_w increases. In the American specification shear lag factor U is taken as unity for $L_w \geq 1.3D$ and in the Canadian specification this limiting value is given as $L_w \geq 2.0w$ or assuming $w = \pi.(D/2)$ this value becomes $L_w \geq 1.57D$. Therefore a more conservative limit is adopted in the Canadian specification. For weld lengths smaller than the smallest specified limits for shear lag i.e., $L_w \geq 1.0D$ in ANSI/AISC (2010) and $L_w \geq 1.0w$ in CAN/CSA-S16 (2009) specifications, the collapse behaviour tends to be governed by a block shear type of failure. In between these upper and lower limits design equations are given for the calculation of shear lag coefficient, U.

The design of structural stainless steel members and connections are covered in Eurocode 3 - Design of steel structures - Part 1-4: General rules - Supplementary rules for stainless steels

Table 5 Design provisions for shear lag in hollow sections with slotted end connection with single welded concentric gusset plate

Specification	Shear lag coefficient, U	Validity range
CHS ANSI/AISC (2010)	$U = 1 - \dfrac{\bar{x}}{L_w}$ for $1.3D > L_w \geq D$ $U = 1$ for $L_w \geq 1.3D$ (*CHS only*)	$L_w \geq D$
SHS ANSI/AISC (2010)	$U = 1 - \dfrac{\bar{x}}{L_w}$ for $L_w \geq H$ B is the width of SHS section	$L_w \geq H$
CHS & SHS CAN/CSA-S16 (2009)	$U = 1$ for $L_w/w \geq 2.0$ $U = 0.5 + 0.25\,L_w/w$ for $2.0 > L_w/w \geq 1.0$ $U = 0.75\,L_w/w$ for $L_w/w < 1.0$	N.A

Table 6 Design provisions for block shear (tear-out)

ANSI/AISC (2010)	$T_r + V_r = \phi U_{bs} A_{nt} F_u + 0.6\phi A_{gv} F_y \leq \phi U_{bs} A_{nt} F_u + 0.6\phi A_{nv} F_u$ in which $\phi = 0.75$ and $U_{bs} = 1.0$
CAN/CSA-S16 (2009)	$T_r + V_r = \phi A_{nt} F_u + 0.6\phi A_{gv} F_y \leq \phi A_{nt} F_u + 0.6\phi A_{nv} F_u$ in which $\phi = 0.9$
EN1993-1-8 (2005)	$T_r + V_r = \dfrac{1}{\gamma_{M2}} A_{nt} F_u + \dfrac{1}{\gamma_{M0}}\dfrac{1}{\sqrt{3}} A_{nv} F_y \qquad \gamma_{M0} = 1.0, \quad \gamma_{M2} = 1.25$

Table 7 Comparison of test strengths with code predicted nominal resistance values for carbon steel

Specimen	Test		Design				Failure mode	
	N_{test} (kN)	N_{YCP} (kN)	GY	PF		TO	Design failure ode	Test failure mode
			$A_g.F_y$ (kN)	$A_e.F_u$ (kN)		AISC, CSA, EC3 V_r (kN)		
				AISC	CSA			
C-L30-NW	103.0	77	176.9	-	59.4	54.7	TO	TO
C-L45-NW	135.4	101	176.9	-	89.0	82.1	TO	TO
C-L60-NW	161.9	138	176.9	-	118.7	109.4	TO	TO
C-L76-NW	192.3	157	176.9	188.0	150.6	138.8	TO	CF
C-L90-NW	190.3	142	176.9	201.6	178.1	164.2	TO	CF
C-L105-NW	187.4	150	176.9	275.8	207.2	191.5	GY	CF
C-L30-RW	157.0	117	176.9	-	68.1	95.5	CF (CSA)	TO
C-L45-RW	184.4	132	176.9	-	102.2	122.9	CF (CSA)	TO
C-L60-RW	215.8	163	176.9	-	136.3	150.2	CF (CSA)	TO
C-L76-RW	241.3	195	176.9	215.8	172.9	179.6	CF (CSA)	CF
C-L90-RW	247.2	191	176.9	231.4	204.4	205.0	GY	CF
C-L105-RW	251.1	215	176.9	316.6	237.8	232.3	GY	CF
S-L30-NW	121.6	91	204.1	-	59.6	54.7	TO	TO
S-L45-NW	149.1	115	204.1	-	89.4	82.1	TO	TO
S-L60-NW	192.3	157	204.1	-	119.3	109.4	TO	TO
S-L70-NW	251.1	184	204.1	202.8	139.1	127.7	TO	CF
S-L90-NW	251.1	193	204.1	229.8	178.9	164.2	TO	CF
S-L105-NW	288.4	229	204.1	243.3	208.7	191.5	TO	CF
S-L30-RW	147.2	103	204.1	-	67.1	95.5	CF (CSA)	TO
S-L45-RW	188.4	135	204.1	-	100.7	122.9	CF (CSA)	TO
S-L60-RW	225.6	161	204.1	-	134.3	150.2	CF (CSA)	TO
S-L70-RW	274.7	214	204.1	228.3	156.6	168.5	CF (CSA)	CF
S-L90-RW	314.9	256	204.1	258.7	201.4	205.0	CF (CSA)	CF
S-L105-RW	321.8	272	204.1	273.9	235.0	232.3	GY	CF

F_y = 380 MPa, F_u = 680 MPa
GY: Gross Yield; PF: Peripheral Fracture; TO: Tear-Out

(EN1993-1-4 2006) and the American ASCE Specification for the Design of Cold-Formed Stainless Steel Structural Members, SEI/ASCE (2002). In both specifications, no specific rules exist which cover the design of slotted end tension connections with welded gusset plate.

Table 7 presents code estimations for the test specimens using the expressions given in Tables 5 and 6 for shear lag and tear-out failure modes. In this table test peak loads (N_{test}) and yield capacity strengths (N_{YCP}) are also given for comparison with the code strengths. Note that the code values are all nominal values i.e., partial safety factors were set to unity. Also note that these values were calculated using the material property values given earlier in the paper for yield stress and ultimate tensile stress. In this table code estimations for failure modes (i.e., the governing

mode of failure) are compared with the experimentally achieved modes. As mentioned earlier depending on the weld length, L_w, all the tested connections failed in either a perfect peripheral fracture or a combination of peripheral fracture and a tear-out type of failure mode. Therefore comparing the code failure modes with the test modes in Table 7, in general a close agreement seems to be achieved for short and medium weld lengths. In the test program no specimen failed in a gross-section yielding mode. For the long weld lengths (L_w = 90 mm and 105 mm) the codes estimate gross-section yielding which is not in line with the test findings. Comparing both the test peak and YCP strength levels with nominal code predicted strength values it is observed that the code values are conservative particularly for short and medium weld lengths. In Table 7 for clarity the governing design strengths are highlighted in gray.

As stated earlier the resistance in fracture of an effective section area (A_e) within the connection region is given by $P_n = F_u.A_e$. In codified design the effective area is used to determine the efficiency of the connection under the effects of shear lag and calculated by using a shear lag reduction coefficient, U. As explained above, in the test program for all the specimens the behaviour was mostly controlled by fracture of an effective section resulting in a peripheral fracture or a combination of peripheral and a tear-out type of fracture. Hence it seems reasonable to calculate experimentally obtained shear lag reduction factors and compare them with the code estimated factors. For this purpose, Fig. 12 presents, for all the tested connections, reduction
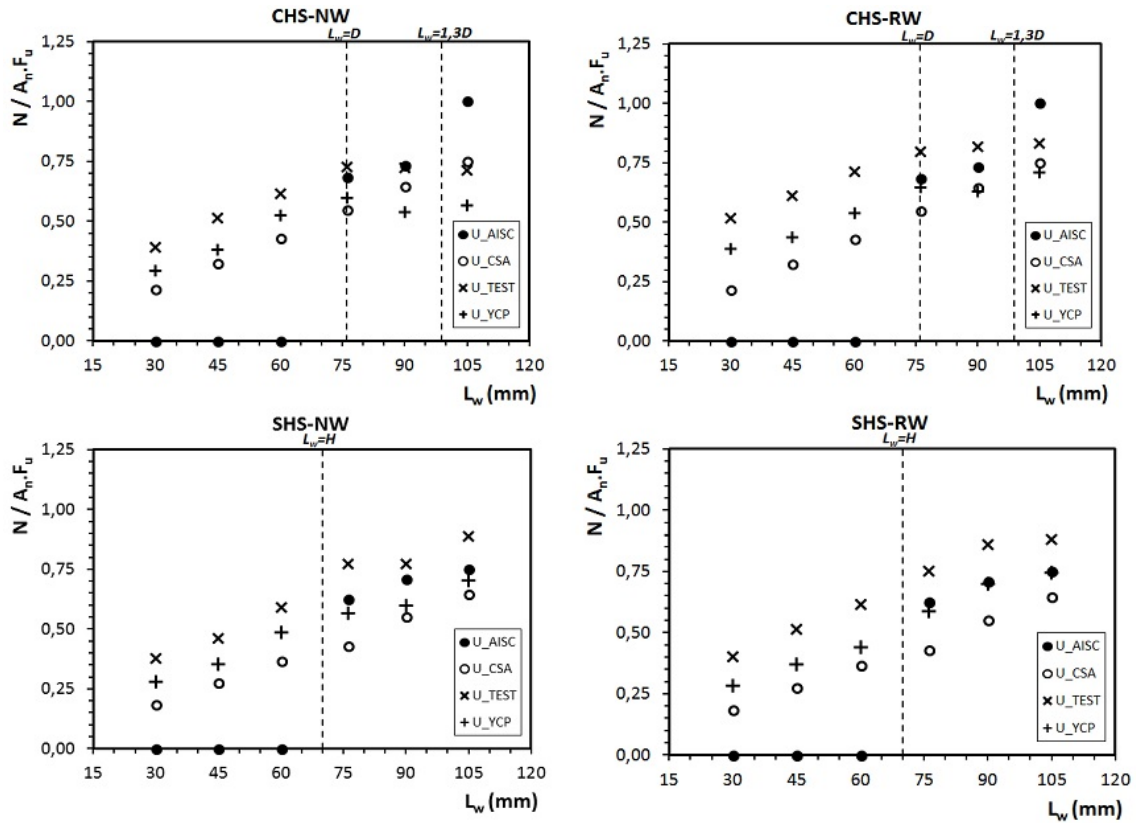

Fig. 12 Comparison between the test and code predicted efficiency factors for all the test specimens

factors given by codes and obtained from tests. In the plots shear lag factors estimated by AISC and CSA codes are given and compared with test reduction factors which are calculated by dividing the test strength by the analytical fracture strength of a net section with full section efficiency, i.e., $U = 1$ ($A_n.F_u$). This ratio is given on the vertical axis of the plots as $N/A_n.F_u$. Two test strength levels were used for the calculation of the test reduction factors denoted on the plots by U_TEST and U_YCP which correspond to the test peak strength (N_{test}) and the yield capacity strength (N_{YCP}) levels, respectively. Note again that the Canadian CSA code covers all the test geometries (i.e., weld length ratios) studied in the test program whereas the validity range for the weld length ratio in the American AISC code is limited. In Fig. 12, it is observed in general that strength reduction factors based on the test strengths (both N_{test} and N_{YCP}) follow similar trends with particularly the Canadian CSA code factors. Reductions factors based on the test peak strengths (U_TEST) are higher than those based on the yield capacity strengths (U_YCP).

The results indicate that using the Canadian CSA reduction factors for the design of slotted end connections in stainless steel might be reasonable and safe. It should be noted that since the deformation levels at the test peak loads are very high using the reduction factors which correspond to the yield capacity load and deformation levels could be recommended for a better design.

5. Conclusions

In this paper, shear lag induced failure of slotted end tension connections is investigated for circular and square hollow section members in stainless steel. An experimental program was carried out on 24 slotted gusset plate welded stainless steel circular and square member end connections under axial tension. Two parameters that were considered as variables in the test program were the fillet weld length L_w and the end condition of the welded gusset plate inside the slot being welded or non-welded.

For the specimens in the test program having a range of weld lengths between 30mm and 105 mm no gross-section yielding was observed. On the other hand most of the specimens were observed to fail by peripheral fracture (PF) due to shear lag. Specimens with longer weld lengths (particularly $L_w = 90$ mm and $L_w = 105$ mm) exhibited a nearly perfect peripheral fracture of the whole circular/square hollow cross section with crack propagating around the member periphery. For the specimens with short and medium weld lengths (L_w between 30 mm and 70 mm) peripheral fracture which initiated at the slotted end and gusset plate juncture seemed later to interact with a tear out type of behaviour.

Load-displacement response curves for the specimens were plotted and comparisons were made mainly between the RW and NW cases. For all RW specimens a sudden drop in strength is observed right after the maximum load is achieved whereas for the NW specimens a smooth transition is noted. With this respect, a more ductile behavior is observed for the specimens with their slotted ends un-welded to the gusset plate. In general the RW specimens reached higher ultimate loads than the NW specimens but at higher elongation levels.

The maximum strength and yield capacity strength results obtained from the test program were compared with currently available design guidance for slotted gusset plate welded tubular end connections. It is noted that no specific rules exist in international specifications on structural stainless steel which cover the design of such connections. Therefore, the results of this study were compared with the design rules for carbon steel. Based on the observation that the connections

exhibited large deformations at test peak strengths a reduced level of strength corresponding to a first yield point on the load-displacement curves was used for comparison with design. First yield points namely the yield capacity points (YCPs) were achieved for more practical and serviceable deformation levels. Comparing both the test peak and YCP strength levels with nominal code predicted strength values it was observed that the code values are conservative particularly for short and medium weld lengths.

Reduction in strength due to shear lag is taken into account in design codes by using a so called shear lag reduction factor, U. Reduction factors obtained by using the test strength values were also compared with the factors given by codes for the range of weld lengths considered in the test program. Particularly the test reduction factors based on the yield capacity strengths were in closer agreement with the factors proposed by the Canadian CSA code. This agreement was achieved for all the specimens in the test program. The results indicate that using the Canadian CSA reduction factors for the design of slotted end tubular connections in stainless steel might be reasonable and safe. Therefore, this research has provided evidence for the possible recommendation for use of the current Canadian design formulations for carbon steel to be applied to the design of slotted gusset plate welded CHS and SHS tension connections in stainless steel.

References

Afshan, S. and Gardner, L. (2013), "The continuous strength method for structural stainless steel design", *Thin-Wall. Struct.*, **68**, 42-49.

ANSI/AISC 360 (2010), *Specification for Structural Steel Buildings*, American Institute of Steel Construction (AISC), Chicago, IL, USA.

Aoki, H. (2000), "Establishment of design standards and current practice for stainless steel structural design in Japan" *Journal of Constructional Steel Research*, **54**(1), 191-210.

Baddoo, N. (2008), "Stainless steel in construction: A review of research, applications, challenges and opportunities", *J. Construct. Steel Res.*, **64**(11), 1199-1206.

Becque, J., Lecce, M. and Rasmussen, K.J.R. (2008), "The direct strength method for stainless steel compression members", *J. Construct. Steel Res.*, **64**(11), 1231-1238.

Burgan, B.A., Baddoo, N.R. and Gilsenan, K.A. (2000), "Structural design of stainless steel members: comparison between Eurocode 3, Part 1.4 and tests results", *J. Construct. Steel Res.*, **54**(1), 51-73.

CAN/CSA-S16 (2009), *Limit States Design of Steel Structures*, Toronto Canadian Standards Association (CSA).

Di Sarno, L., Elnashai, A.S. and Nethercot, D.A. (2006), "Seismic retrofitting of framed structures with stainless steel", *J. Construct. Steel Res.*, **62**(1-2), 93-104.

EN1993-1-8 (2005), *Eurocode 3 Design of Steel Structures – General Rules — Part 1-8*: *Design of Joints*, European Committee for Standardization, Brussels, Belgium.

EN1993-1-4 (2006), *Eurocode 3 Design of Steel Structures – Part 1-4*: *General Rules – Supplementary Rules for Stainless Steels*, European Committee for Standardization, Brussels, Belgium.

Feng, R. and Young, B. (2011), "Design of cold-formed stainless steel tubular T- and X-joints", *J. Construct. Steel Res.*, **67**(3), 421-436

Huang, Y. and Young, B. (2013), "Tests of pin-ended cold-formed lean duplex stainless steel columns", *J. Construct. Steel Res.*, **82**, 203-215.

Johansson, B. and Olsson, A. (2000), "Current design practice and research on stainless steel structures in Sweden", *J. Construct. Steel Res.*, **54**(1), 3-29.

Korol, R.M. (1996), "Shear lag in slotted HSS tension members", *Can. J. Civil Eng.*, **23**(6), 1350-1364.

Kouhi, J., Talja, A., Salmi, P. and Ala-Outinen, T. (2000), "Current R&D work on the use of stainless steel in construction in Finland", *J. Construct. Steel Res.*, **54**(1), 31-50.

Ling, T.W., Zhao, X.L., Al-Mahaidi, R. and Packer, J.A. (2007), "Investigation of shear lag failure in gusset plate welded structural steel hollow section connections", *J. Construct. Steel Res.*, **63**(3), 293-304.

Martinez-Saucedo, G. and Packer, J.A. (2009), "Static design recommendations for slotted end HSS connections in tension", *J. Struct. Eng., ASCE*, **135**(7), 797-805.

Martinez-Saucedo, G., Packer, J.A. and Christopoulos, C. (2008), "Gusset plate connections to circular hollow section braces under inelastic cyclic loading", *J. Struct. Eng., ASCE*, **134**(7), 1252-1258.

Martinez-Saucedo, G., Packer, J.A. and Willibald, S. (2006), "Parametric finite element study of slotted end connections to circular hollow sections", *Eng. Struct.*, **28**(14), 1956-1971.

Nethercot, D.A., Salih, E.L. and Gardner, L. (2009), "Behaviour and design of stainless steel bolted connections", *Proceedings of the 3rd International Forum on Advances in Structural Engineering*, Shanghai, China, November, pp. 1-18.

Ramberg, W. and Osgood, W.R. (1943), "Description of stress–strain curves by three parameters", Technical Note No. 902, National Advisory Committee for Aeronautics, Washington, D.C., USA.

Rasmussen, K.J.R. (2003), "Full-range stress-strain curves for stainless steel alloys", *J. Construct. Steel Res.*, **59**(1), 47-61.

Rasmussen, K.J.R., Burns, T. and Bezkorovainy, P. (2004), "Design of stiffened elements in cold-formed stainless steel sections", *J. Struct. Eng. – ASCE*, **130**(11), 1764-1771.

Roger Cheng, J.J., Kulak, G.L. and Khoo, H.A. (1998), "Strength of slotted tubular tension members", *Can. J. Civil Eng.*, **25**(6), 982-991.

Rossi, B. and Rasmussen, K.J.R. (2013), "Carrying capacity of stainless steel columns in the low slenderness range", *J. Struct. Eng. – ASCE*, **139**(6), 1088-1092.

Salih, E.L., Gardner, L. and Nethercot, D.A. (2013), "Numerical study of stainless steel gusset plate connections", *Eng. Struct.*, **49**, 448-464.

SEI/ASCE (2002), 8-02, *Specification for the Design of Cold-Formed Stainless Steel Structural Members*, American Society of Civil Engineers.

Theofanous, M. and Gardner, L. (2012), "Effect of element interaction and material nonlinearity on the ultimate capacity of stainless steel cross-sections", *Steel Compos., Struct., Int. J.*, **12**(1), 73-92.

Willibald, S. and Martinez-Saucedo, G. (2006), "Behaviour of gusset plate connections to ends of round and elliptical hollow structural section members", *Can. J. Civil Eng.*, **33**(4), 373-383.

Young, B. (2008), "Experimental and numerical investigation of high strength stainless steel structures", *J. Construct. Steel Res.*, **64**(11), 1225-1230.

DL